Chemistry–A European Journal
Research Article
doi.org/10.1002/chem.202200005
Chemistry Europe
European Chemical Societies Publishing
www.chemeurj.org

Induced Near-Infrared Emission and Controlled Photooxidation based on Sulfonated Crown Ether in Water

Xiaoyun Dong,[a] Cong Zhang,[a] Xianyin Dai,[a] Qi Wang,[a] Ying-Ming Zhang,*[a] Xiufang Xu,[a] and Yu Liu*[a]

Abstract: Regulation of physio-chemical properties and reaction activities via noncovalent methodology has become one of increasingly significant topics in supramolecular chemistry and showed inventive applications in miscellaneous fields. Herein, we demonstrate that sulfonated crown ether can form very stable host-guest complexes with a series of push-pull-type photosensitizers, eventually leading to the dramatic fluorescence enhancement in visible and near-infrared regions. Meanwhile, severe suppression in singlet oxygen ($^1O_2$) production is found, mainly due to the higher energy barriers between the excited single and triple states upon host-guest complexation. Moreover, such complexation-induced tuneable $^1O_2$ generation systems has been utilized in adjusting the photochemical oxidation reactions of polycyclic aromatic hydrocarbons (anthracene) and sulfides ((methylthio)benzene) in water. This supramolecularly controlled photooxidation based on the selective molecular binding of crown ether with photosensitizers may provide a feasible and applicable strategy for monitoring and modulating many photocatalysis processes in aqueous phase.

Introduction

As a type of frequently encountered reactive oxygen species (ROS), the photochemically generated singlet oxygen ($^1O_2$) via photosensitizer-mediated intersystem crossing (ISC) has continuously simulated an upsurge of interest, mainly due to its immense advantages in phototheranostics and photocatalysis.[1] Since spectroscopic activities of a given optical agent are largely dependent on the electronic transition among different states of excitions, molecular design through chemically synthetic methods has been proven as a direct and effective method to alter the distribution of ROS (including $^1O_2$) in both inanimate milieu and physiological environment.[2] However, besides the maximization of $^1O_2$ efficiency by molecular design, it is highly imperative to generate $^1O_2$ in a precise and controllable manner, because the inadvertent photosensitizer activation and 'always-on' $^1O_2$ production can make adverse effects and severely hamper its practical applications.[3]

Supramolecular chemistry based on cavity-bearing macrocycles has provided a powerful strategy to regulate the physicochemical performance of self-assembled superstructures. By leveraging the noncovalent interactions, one can optimize molecular configuration, aggregate states, and photoluminescence behaviors, with the final goal of attaining nanoscaled assemblies and materials with elaborate functions.[4] In particular, the host-guest complexation between photosensitizers and well-crafted artificial receptors, such as cyclodextrins,[5] calixarenes,[6] cucurbiturils,[7] and pillararenes,[8] has shown great superiorities in tuning the radiative emission and nonradiative relation processes,[9] thus endowing supramolecular assembled architectures with desired $^1O_2$ generation capacity. In this regard, compared to other classic macrocycles, the research on the supramolecularly tunable $^1O_2$ generation using crown ethers is unevenly developed, and there is a relative paucity of studies on the crown ether-controlled $^1O_2$ generation in aqueous solution. This is attributed to the assumption that the conventional crown ethers merely possessing alkoxyl rings are prone to entrap small-sized metal ions and secondary alkylammonium salts in organic solution rather than the large-sized π-aromatic photosensitizers in water.[10]

Recently, we have developed some types of water-soluble crown ethers, which are composed of two sulfonated phenyl or naphthyl cores connected by alkoxyl chains. These structural features can ensure strong host-guest complexation with bulky π-conjugated (bi)pyridinium salts via synergistic electrostatic and π-stacking interactions.[11] In this study, bis(4,8-disulfonato-1,5-naphtho)-32-crown-8 (DNC) is first employed to tightly encapsulate a series of triphenylamine-containing pull-push-type photosensitizers, accompanied by the dramatic fluorescence enhancement, especially in the near-infrared (NIR) region, as a result of the conformational fixation by crown ether. More significantly, due to the decreased energy barrier in singlet-triplet transition, it is also found that the $^1O_2$ production efficiency and concomitant photooxidation abilities of obtained photosensitizers toward anthracene and (methylthio)benzene can be greatly suppressed upon complexation with DNC. This uncommon controlled photooxidation based on the selective molecular binding with crown ethers in water will greatly

[a] X. Dong, C. Zhang, X. Dai, Q. Wang, Dr. Y.-M. Zhang, Prof. Dr. X. Xu, Prof. Dr. Y. Liu
College of Chemistry
State Key Laboratory of Elemento-Organic Chemistry
Nankai University, Tianjin 300071 (P. R. China)
E-mail: ymzhang@nankai.edu.cn
yuliu@nankai.edu.cn

Supporting information for this article is available on the WWW under https://doi.org/10.1002/chem.202200005

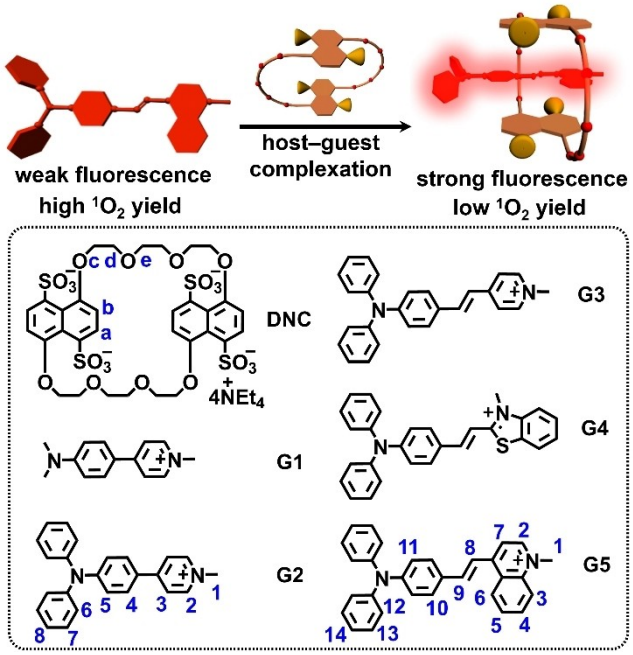

Scheme 1. Chemical structures of host and guest molecules, proton designation, and schematic illustration of the DNC-mediated $^1O_2$ generation in water for the controlled photooxidation of anthracene and (methylthio)benzene.

extend the applicability of supramolecular methodology in the manipulation of photophysical dissipation pathways for optimal theranostic approaches and improved catalytic technology.

Results and Discussion

The molecular binding behaviors between DNC and five push-pull-type molecules (G1-G5) for the controlled $^1O_2$ production are illustrated in Scheme 1. The guest molecules G1 and G2 were synthesized by the Suzuki–Miyaura coupling reactions followed by the methylation of pyridyl group with iodomethane.[12] The guest molecules G3-G5 were synthesized by the Knoevenagel condensation of aldehyde-bearing triphenylamine with *N*-methyl pyridinium, benzothiazolium, and quinolinium salts, respectively (Figures S1–S3, Supporting Information).[13] Given that well-defined photosensitizers are believed as the indispensable components in achieving the $^1O_2$ production with high yield, triphenylamine and *N*-methylated organic cations have been introduced as donor and acceptor groups, respectively, to adjust the whole π-conjugation and push-pull balance in these guest molecules (G2-G5). Next, the molecular binding behaviors in the ground state were investigated by the ^{1}H NMR titrations. As shown in Figure 1a, the pyridinium's $H_{2\text{-}4}$ protons in G2 underwent obvious downfield shift, whereas the remaining triphenylamine's $H_{6\text{-}8}$ protons showed pronounced upshift upon host-guest complexation with DNC, accompanied by the broadening of DNC's resonance peaks, which is contributed to the strong mutual shielding

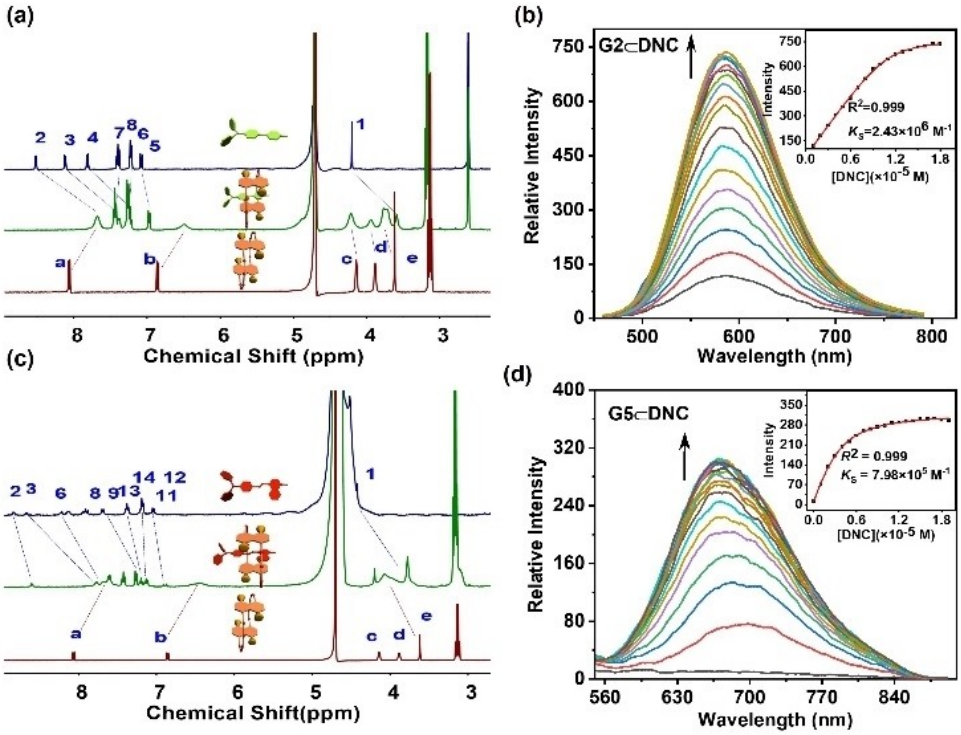

Figure 1. ^{1}H NMR spectra (400 MHz, D_2O, 298 K) of (a) G2 and (c) G5 in the presence of DNC ([G2] = [G5] = [DNC] = 1.0×10^{-3} M). Fluorescence spectral titration and K_a calculation (insert curves) of (b) G2⊂DNC and (d) G5⊂DNC complexation ([G2] = [G5] = 1.0×10^{-5} M, and [DNC] = 0-1.8×10^{-5} M).

effect between the naphthyl ring and the cationic backbone. Similarly, the proton signals of pyridinium and methyl groups of G5 ($H_{1\text{-}3,\ 6}$) also showed large upfield shifts in the presence of DNC (Figure 1c). These results demonstrate that the sulfonated DNC is prone to encapsulate the pyridinium heads through the favorable π-stacking and electrostatic interactions.

Subsequently, the photophysical properties of these obtained inclusion complexes with DNC were preliminarily examined by fluorescence spectroscopy. As can be seen from Figure 1b, 1d, and Figures S4–S6 (Supporting Information), the fluorescence intensity of G1-G5 was dramatically enhanced upon addition of DNC, indicative of their close intermolecular communication in the excited state. In addition, the complexation-induced fluorescence enhancement could be conveniently distinguished by the naked eyes; that is, an equimolar mixture of sulfonated crown ether DNC with organic cations G1-G5 gave intense fluorescence emission from bright yellow to red upon exposure to light irradiation (Figure S7, Supporting Information). It is also noteworthy that despite of a slight hypochromatic shift, NIR fluorescence emission was eventually observed at 675 nm in the case of G5⊂DNC complexation (Figure 1b).

Next, the plot of fluorescence intensity changes against the molecular fraction gave an inflection point at 0.5, suggesting the 1:1 binding stoichiometry for the host-guest complexation (Figures S8-S11, Supporting Information). After further validating the 1:1 binding stoichiometry in all the cases of inclusion complexes, the binding association constants (K_a) were accordingly calculated in the range of 10^5–10^6 M^{-1} order of magnitude in water by the nonlinear least-squares curve-fitting method (Figure 1b, 1d and Figures S4-S6, Supporting Information). Since DNC is a negatively charged receptor with an electron rich cavity, the binding stability of DNC is largely dependent on the positive-charge numbers and the π-conjugation of pyridinium guests. In our case, the guest molecules possessed the same triphenylamine and a singly charged group, which could give rise to the similar binding strengths. In addition, the formation of 1:1 host-guest complexes was further confirmed by electrospray ionization-mass spectrometry. The *m/z* peaks at 539.0923, 400.4028, 409.0746, 427.7320, and 425.7466 could be clearly assigned to $[DNC+G1+H^+]^{2-}/2$, $[DNC+G2]^{3-}/3$, $[DNC+G3]^{3-}/3$, $[DNC+G4]^{3-}/3$, and $[DNC+G5]^{3-}/3$, respectively (Figures S12–S16, Supporting Information). Apparently, the tight and stable host-guest complexation would facilitate the regulation of spectroscopic performance and concomitant $^1O_2$ generation, as described below.

To better understand the mechanisms on complexation-induced fluorescence enhancement, the molecular conformations and excited energies of free guests and their inclusion complexes were calculated by the DFT and TDDFT methods.[14] Taking G4 and G4⊂DNC complex as examples, the dihedral angles (C_A-C_B-C_C-C_D) were obtained as −179.6° and −179.3° in the ground states (S_0) of G4 and G4⊂DNC complex, respectively (Figure 2a and 2b), indicating that the G4 molecule still retained the coplanar structures when encapsulated in the DNC cavity. While the diphenyl aniline moiety of G4 was not fully accommodated in the DNC cavity, extensive hydrogen-bonding

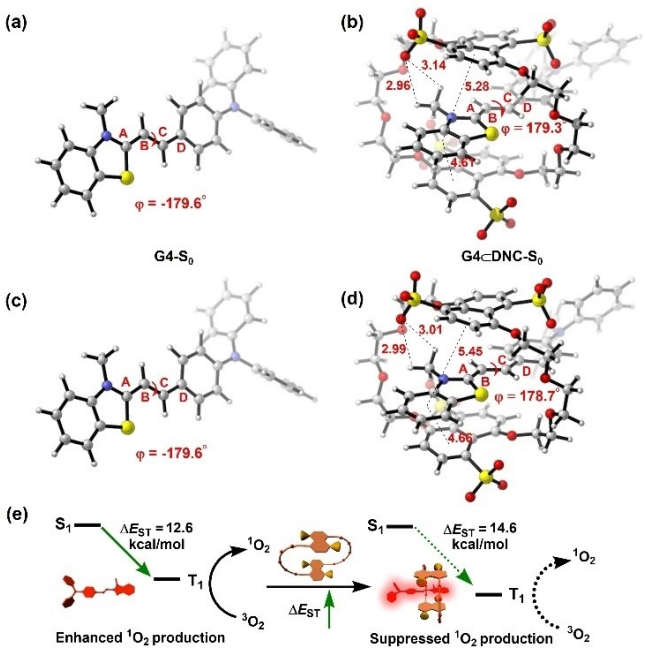

Figure 2. DFT and TDDFT calculation on optimized geometries of (a, c) free G4 and (b, d) G4⊂DNC complex in the (a, b) ground and (c, d) first excited singlet states. The negative dihedral angle ϕ(C_A–C_B–C_C–C_D) means that the benzothiazole ring rotates clockwise relative to the diphenyl aniline ring along the central C_B–C_C bond. (e) Energy barrier diagram of free G4 molecule and G4⊂DNC complex with oxygen.

interconnection was observed between the benzothiazolyl moiety and the sulfonate site of DNC with O···H distances of 2.96 and 3.14 Å. Moreover, the interplanar distances between G4's benzothiazolyl and DNC's naphthyl rings were measured as 4.61 and 5.28 Å, corresponding to the existence of strong π-stacking interaction. Thus, it is believed that the efficient π-stacking and hydrogen-bonding interactions turned out to play major roles in maintaining the stability of the inclusion complex.

Moreover, the stable molecular conformations of G4 and G4⊂DNC complex were also calculated in their first excited singlet states (S_1) (Figure 2c and 2d). Compared to the dihedral angles of G4 in the S_0 state, the ones in the S_1 state were almost unchanged and G4 still maintained a coplanar conformation. Meanwhile, the calculation also demonstrated that in the S_0 state, the energy barriers for chemical-bond rotation, especially for the double bonds, were so large (ranging from 7.4 to 28.7 kcal/mol) that it could hardly occur under moderate condition (Figures S17–S18, Supporting Information). In comparison, the energy barriers became smaller to some extent upon excitation, but the coplanar structure was still the most stable configuration of G4 in the S_1 state (Figure S19, Supporting Information). Although the host-guest interaction with DNC could not make significant impact on the conformational change of G4, the rotational dissipation of energy might be prohibited upon host-guest complexation. In view of the planar conformation of G4 before and after encapsulation in the DNC cavity, the mechanism on complexation-induced fluorescence

enhancement can be ruled out from the twisted intramolecular charge transfer relaxation.

Furthermore, on account of the excellent spectroscopic performance of triphenylamine-based derivatives, the $^1O_2$ generation abilities of these obtained guest dyes (G1-G5) in solution were studied by using 9,10-anthracenediylbis(methylene)dimalonic acid (ABDA) as the detecting probe.[15] As discerned from Figure 3a, the UV-Vis absorbance intensity of ABDA gradually decreased in the presence of free G5 under the continuous light irradiation. In contrast, no such decrease was observed in the case of G5⊂DNC complex (Figure 3b). Meanwhile, no obvious change in the UV-Vis absorbance of ABDA was observed with or without DNC under the light irradiation, implying the ROS generation was greatly inhibited upon host-guest complexation with DNC (Figure S20, Supporting Information). Accordingly, the degradation percentage of ABDA largely decreased in the presence of DNC, due to the inhibition of $^1O_2$ generation (Figure 3c and 3d). In addition, by comparing the integral area in absorbance spectra and using tris(2,2′-bipyridyl)-ruthenium(II) chloride as the standard, the $^1O_2$ quantum yield of G5 was calculated as high as 146%, whereas this value sharply decreased to only 8.8% after complexation with DNC (Figure S21 and Table S1, Supporting Information). The $^1O_2$ generation abilities of G1-G4 were also investigated, giving a very similar complexation-induced inhibition effect and the structure-dependent $^1O_2$ generation abilities (Figures S22–S25, Supporting Information).

Subsequently, quantum chemical calculations have also been performed to illuminate the regulation mechanism on $^1O_2$ generation. It is known that after absorbing light, photosensitizers can be excited from S_0 state to S_1 state and then to the lowest excited triplet state (T_1) via the relaxation process of ISC pathway. Then, the energy is transferred to the ground state oxygen ($^3O_2$) and ROS is accordingly generated. The ISC efficiency of a sensitizer is inversely proportional to the energy barrier (ΔE_{ST}) between S_1 and T_1 states and reducing ΔE_{ST} is an effective strategy to achieve fluorescence enhancement.[16] In our case, the ΔE_{ST} value of G4 alone is 12.6 kcal/mol, whereas this value increased to 14.6 kcal/mol in the presence of DNC (Figure 2e). That means, the ISC process of G4⊂DNC complex becomes difficult to take place and the $^1O_2$ production is thus suppressed. Therefore, the radiative emission from S_1 to S_0 state emerges to be the predominant pathway and the fluorescence intensity of the inclusion complex is enhanced. These calculated results are well consistent with the spectroscopic data.

Considering the tunable $^1O_2$ generation by the inclusion complexation with DNC, we were curious to know whether such conversion could be utilized to control the $^1O_2$-invloved photochemical reactions. It is known that thioether and anthryl derivatives could be easily oxidized by photosensitizers under light irradiation at a given wavelength. Thus, the photooxidation of (methylthio)benzene and anthracene were chosen as the model reactions to investigate the controllable catalytic performance of obtained supramolecular complexes. On ac-

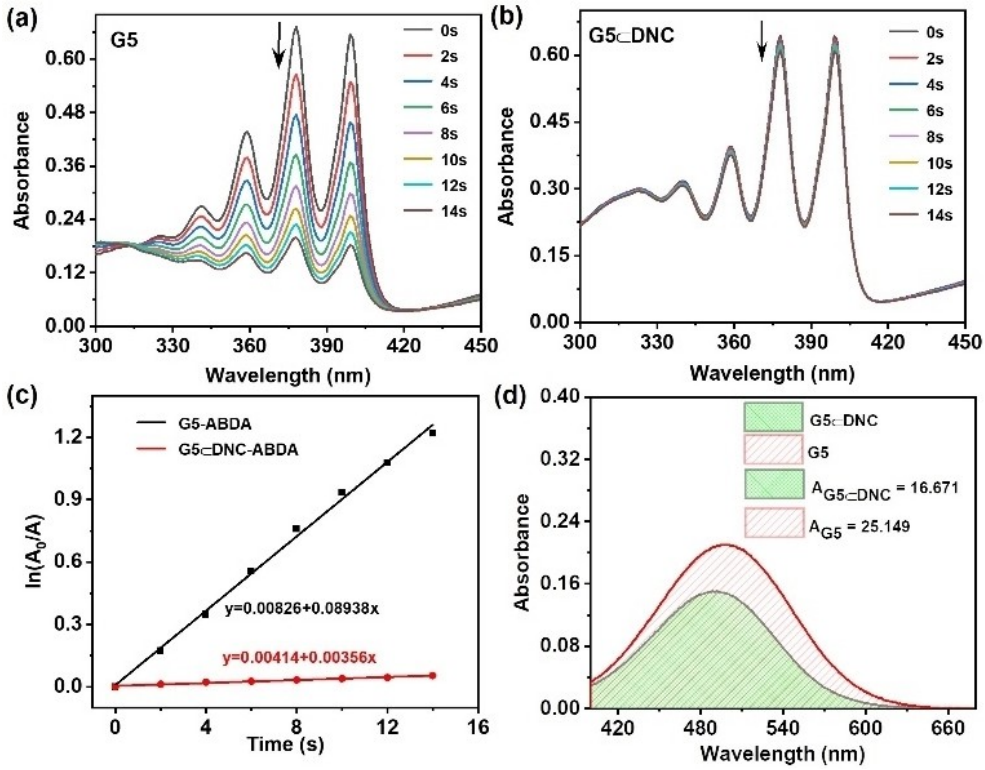

Figure 3. UV-Vis spectra of ABDA in the presence of (a) G5 and (b) G5⊂DNC complex under white light irradiation ($\lambda > 420$ nm, 220 mW/cm^2; (c) Normalized degradation percentages of ABDA at 378 nm in the presence of G5 and G5⊂DNC under white light irradiation ($\lambda > 420$ nm, 220 mW/cm^2); (d) UV-Vis spectral integral area of G5 and G5⊂DNC complex ([G5] = 1×10^{-5} M, [DNC] = 1×10^{-5} M and [ABDA] = 5×10^{-5} M).

count of the highest $^1O_2$ production efficiency, G5 was used as the photosensitizer to generate $^1O_2$ under visible light irradiation ($\lambda > 420$ nm). As can be seen from Figure 4a, (methylthio)-benzene was largely consumed in the presence of G5, accompanied by the obvious decrease in UV-Vis absorbance in the range of 340–400 nm. However, no such decrease was observed in the case of G5⊂DNC complex (Figure 4b). Accordingly, the conversion ratios of photooxidation reaction could be conveniently recorded by comparing the integral areas of methyl groups in (methylthio)benzene and (methylsulfinyl)-benzene at 2.42 and 2.80 ppm, respectively. As discerned from Figure S26 (Supporting Information), 91.7% of (methylthio)-benzene was converted to (methylsulfinyl)benzene with G5 upon light irradiation for 5 h, whereas this value decreased to only 37.9% with G5⊂DNC complex under the same experimental condition. In the control experiments, the conversion efficiency of (methylthio)benzene was 36.9% and 25.2% in the presence and absence of DNC, respectively (Figure S27, Supporting Information). These results suggest that the photosensitizing ability of G5 could be completely inhibited by the complexation with DNC.

Similar controllable photooxidation could also take place using anthracene as the reactant. As shown in Figure 4c, the UV-Vis absorbance intensity of anthracene gradually decreased upon addition of photosensitizer but the UV-Vis absorbance was hardly changed when G5 or G5⊂DNC complex was irradiated alone in the range of 320–420 nm (Figure S28, Supporting Information), jointly indicative of photooxidation conversion of pristine anthracene. The *m/z* peak at 208.05171 in mass spectrum could be clearly assigned to anthraquinone as the photooxidation product (Figure S29, Supporting Information). In keen contrast, the decrease in UV-Vis absorbance was suppressed to great extent when DNC was added, apparently due to the host-guest-complexation-induced inhibition on $^1O_2$ production (Figure 4d). These results demonstrate that the $^1O_2$ generation efficiencies of photosensitizers and the conversion of photooxidation reactions could be significantly suppressed upon complexation with DNC (Figure 4e and 4f).

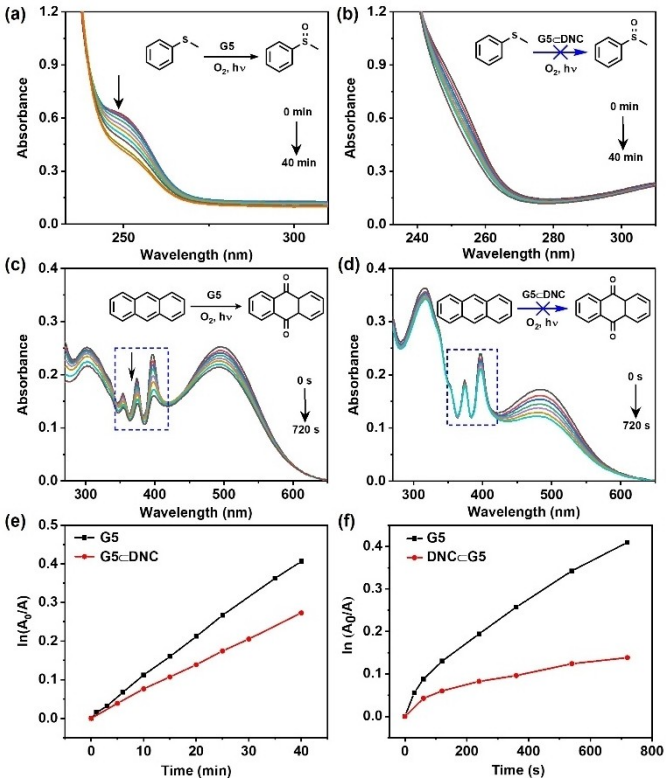

Figure 4. UV-Vis spectral changes of (a, b) (methylthio)benzene and (c, d) anthracene in the presence of (a, c) free G5 and (b, d) G5⊂DNC complex. Normalized degradation percentages of (e) (methylthio)benzene at 250 nm and (f) anthracene at 374 nm in presence of G5 and G5⊂DNC complex ([G5] = [DNC] = 1×10^{-5} M and [(methylthio)benzene] = [anthracene] = 1.3×10^{-4} M).

Conclusion

In conclusion, a series of pull-push-type photosensitizers (G2-G5) have been successfully synthesized using triphenylamine as the donor group, which can form very stable host-guest complexes with DNC. As investigated by the spectroscopic titration experiments and computational studies, the fluorescence emission of G1-G5 can be dramatically enhanced as a result of multiple favorable hydrogen-bonding and π-stacking interactions. Remarkably, the NIR fluorescence enhancement has been realized in the G5⊂DNC complexation. Meanwhile, strikingly distinct $^1O_2$ generation abilities have been achieved by altering the molecular structures of acceptor groups. It is also found that the $^1O_2$ production can be efficiently suppressed once the photosensitizers are encapsulated in the DNC's ring, mainly due to the higher energy barrier between S_1 and T_1 states that can make undesirable effect on $^1O_2$ production. More remarkably, the $^1O_2$-involved photooxidation of anthracene and (methylthio)benzene can be well-tuned by the host-guest complexation with DNC. To be envisaged, this unique crown ether-binding-controlled photooxidation in water can be easily amenable to many other scenarios and may find more versatile applications, such as photochemically assisted biomedical therapies and environmental remediation.

Experimental Section

All the experimental data, including compound characterization, UV-Vis/NMR spectral titration, quantum chemical calculation, and other results in the control experiments, have been provided in the Supporting Information.

Acknowledgements

This work was financially funded by the National Natural Science Foundation of China (grants 21871154, 22171148, 21873051, and 22131008) and the Fundamental Research Funds for the Central Universities, Nankai University.

Conflict of Interest

The authors declare no conflict of interest.

Data Availability Statement

The data that support the findings of this study are available in the supplementary material of this article.

Keywords: host-guest chemistry · photooxidation reaction · singlet oxygen · water-soluble crown ether

[1] a) G. Feng, G.-Q. Zhang, D. Ding, *Chem. Soc. Rev.* **2020**, *49*, 8179–8234; b) W. Zhu, M. Kang, Q. Wu, Z. Zhang, Y. Wu, C. Li, K. Li, L. Wang, D. Wang, B. Z. Tang, *Adv. Funct. Mater.* **2021**, *31*, 2007026; c) P.-P. Jia, L. Xu, Y.-X. Hu, W.-J. Li, X.-Q. Wang, Q.-H. Ling, X. Shi, G.-Q. Yin, X. Li, H. Sun, Y. Jiang, H.-B. Yang, *J. Am. Chem. Soc.* **2021**, *143*, 399–408; d) K. Omoto, S. Tashiro, M. Shionoya, *J. Am. Chem. Soc.* **2021**, *143*, 5406–5412.

[2] a) W. Wu, D. Mao, S. Xu, Kenry, F. Hu, X. Li, D. Kong, B. Liu, *Chem* **2018**, *4*, 1937–1951; b) J. He, Y. Wang, M. A. Missinato, E. Onuoha, L. A. Perkins, S. C. Watkins, C. M. St Croix, M. Tsang, M. P. Bruchez, *Nat. Methods* **2016**, *13*, 263–268.

[3] a) E. Tanrıverdi Eçik, O. Bulut, H. H. Kazan, E. Şenkuytu, B. Çoşut, *New J. Chem.* **2021**, *45*, 16298–16305; b) D. Jia, X. Ma, Y. Lu, X. Li, S. Hou, Y. Gao, P. Xue, Y. Kang, Z. Xu, *Chin. Chem. Lett.* **2021**, *32*, 162–167.

[4] a) X.-Y. Lou, Y.-W. Yang, *J. Am. Chem. Soc.* **2021**, *143*, 11976–11981; b) W.-M. Wang, D. Dai, J.-R. Wu, C.-Y. Wang, Y. Wang, Y.-W. Yang, *Chem. Eur. J.* **2021**, *27*, 11879–11887; c) J. Zhang, H. Qiu, T. He, Y. Li, S. Yin, *Front. Chem.* **2020**, *8*, 560.

[5] a) H. Kitagishi, K. Kano, *Chem. Commun.* **2021**, *57*, 148–173; b) X. Dai, X. Dong, Z. Liu, G. Liu, Y. Liu, *Biomacromolecules* **2020**, *21*, 5369–5379.

[6] a) A. Mazzaglia, N. Angelini, R. Darcy, R. Donohue, D. Lombardo, N. Micali, M. T. Sciortino, V. Villari, L. M. Scolaro, *Chem. Eur. J.* **2003**, *9*, 5762–5769; b) C. Chen, X. Ni, H.-W. Tian, Q. Liu, D.-S. Guo, D. Ding, *Angew. Chem. Int. Ed.* **2020**, *59*, 10008–10012; *Angew. Chem.* **2020**, *132*, 10094–10098; c) H.-T. Feng, Y. Li, X. Duan, X. Wang, C. Qi, J. W. Y. Lam, D. Ding, B. Z. Tang, *J. Am. Chem. Soc.* **2020**, *142*, 15966–15974; d) P. Li, Y. Chen, Y. Liu, *Chin. Chem. Lett.* **2019**, *30*, 1190–1197.

[7] a) F.-F. Shen, Y. Chen, X. Xu, H.-J. Yu, H. Wang, Y. Liu, *Small* **2021**, *17*, 2101185; b) H.-J. Yu, Q. Zhou, X. Dai, F.-F. Shen, Y.-M. Zhang, X. Xu, Y. Liu, *J. Am. Chem. Soc.* **2021**, *143*, 13887–13894; c) J. Robinson-Duggon, F. Pérez-Mora, L. Valverde-Vásquez, D. Cortés-Arriagada, J. R. De la Fuente, G. Günther, D. Fuentealba, *J. Phys. Chem. C* **2017**, *121*, 21782–21789.

[8] a) L. Shao, Y. Pan, B. Hua, S. Xu, G. Yu, M. Wang, B. Liu, F. Huang, *Angew. Chem. Int. Ed.* **2020**, *59*, 11779–11783; *Angew. Chem.* **2020**, *132*, 11877–11881; b) B. Huang, P. Wang, Y. Ouyang, R. Pang, S. Liu, C. Hong, S. Ma, Y. Gao, J. Tian, W. Zhang, *ACS Appl. Mater. Interfaces* **2020**, *12*, 410138–41046; c) W. Qian, M. Zuo, G. Sun, Y. Chen, T. Han, X.-Y. Hu, R. Wang, L. Wang, *Chem. Commun.* **2020**, *56*, 7301–7304.

[9] G. Liu, X. Xu, Y. Chen, X. Wu, H. Wu, Y. Liu, *Chem. Commun.* **2016**, *52*, 7966–7969.

[10] a) H. J. Wang, H.-Y. Zhang, H. Wu, X.-Y. Dai, P.-Y. Li, Y. Liu, *Chem. Commun.* **2019**, *55*, 4499–4502; b) C. Xu, Y. Chen, H.-Y. Zhang, Y. Liu, *J. Photochem. Photobiol. A* **2016**, *331*, 240–246; c) Q. Zhang, F. Chen, X. Shen, T. He, H. Qiu, S. Yin, P. J. Stang, *ACS Macro Lett.* **2021**, *10*, 873–879.

[11] a) L. Chen, Y.-M. Zhang, L.-H. Wang, Y. Liu, *J. Org. Chem.* **2013**, *78*, 5357–5363; b) Y.-M. Zhang, X.-J. Zhang, X. Xu, X.-N. Fu, H.-B. Hou, Y. Liu, *J. Phys. Chem. B* **2016**, *120*, 3932–3940.

[12] P. Yin, T. Wang, Y. Yang, W. Yin, S. Zhang, Z. Yang, C. Qi, H. Ma, *New J. Chem.* **2019**, *43*, 18251–18258.

[13] J. Wang, X. Zhu, J. Zhang, H. Wang, G. Liu, Y. Bu, J. Yu, Y. Tian, H. Zhou, *ACS Appl. Mater. Interfaces* **2020**, *12*, 1988–1996.

[14] a) S. Grimme, J. Antony, S. Ehrlich, H. Krieg, *J. Chem. Phys.* **2010**, *132*, 154104; b) G. Scalmani, M. J. Frisch, B. Mennucci, J. Tomasi, R. Cammi, V. Barone, *J. Chem. Phys.* **2006**, *124*, 94107.

[15] W. Xu, M. M. S. Lee, J.-J. Nie, Z. Zhang, R. T. K. Kwok, J. W. Y. Lam, F.-J. Xu, D. Wang, B. Z. Tang, *Angew. Chem. Int. Ed.* **2020**, *59*, 9610–9616; *Angew. Chem.* **2020**, *132*, 9697–9703.

[16] K. Liu, X. Qiao, C. Huang, X. Li, Z. Xue, T. Wang, *Angew. Chem. Int. Ed.* **2021**, *60*, 14365–14369; *Angew. Chem.* **2021**, *133*, 14486–14490.

Manuscript received: January 2, 2022
Accepted manuscript online: February 7, 2022
Version of record online: ■■, ■■■

RESEARCH ARTICLE

Water-soluble sulfonated crown ether makes very strong host-guest encapsulation with a set of push-pull-type dyes, which can greatly enhance the fluorescence emission from visible to near-infrared regions and significantly suppress the $^1O_2$ generation and concomitant photooxidation ability of photosensitizers in aqueous media.

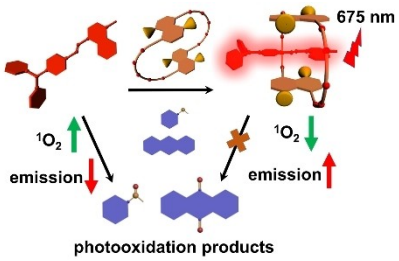

X. Dong, C. Zhang, X. Dai, Q. Wang, Dr. Y.-M. Zhang, Prof. Dr. X. Xu, Prof. Dr. Y. Liu**

1 – 7

Induced Near-Infrared Emission and Controlled Photooxidation based on Sulfonated Crown Ether in Water